Mathl. Comput. Modelling Vol. 18, No. 3/4, pp. 101–113, 1993
Printed in Great Britain.

0895-7177/93 $6.00 + 0.00

Structural Optimization of High Speed Prop Rotors Including Aeroelastic Stability Constraints

A. CHATTOPADHYAY AND T. R. MCCARTHY
Department of Mechanical and Aerospace Engineering, Arizona State University
Tempe, AZ 85287-6106, U.S.A.

J. F. MADDEN, III
Rotorcraft Technology Branch, NASA Ames Research Center
Moffett Field, CA 94035, U.S.A.

Abstract—An optimization procedure is developed to address the problem of aeroelastic stability of high speed prop-rotor aircraft. A composite box beam is used as a perturbational stiffness model and the objective function to be minimized is the perturbational weight. An optimization algorithm, which used the method of feasible directions, is coupled with a hybrid approximate analysis to reduce the computational expense of exact analyses for every function evaluation. The results, compared to a reference rotor which is unstable in both hover and high speed cruise, show significant improvements in the aeroelastic stability without large weight penalties.

1. INTRODUCTION

Recently, there has been a revival of interest in the development of high speed rotor craft that demonstrate cruise aerodynamic efficiencies similar to fixed-wing aircraft and the hovering capabilities of helicopters [1]. The design of this class of aircraft is associated with several critical and often conflicting requirements [2–4]. For example, in order to achieve desirable propulsive efficiencies it is necessary to reduce the tip speed in high speed cruise which causes the rotor to operate at nonideal r.p.m. [4]. This can be overcome through the use of thin airfoils which have high drag divergence Mach numbers (M_{dd}). However, thin airfoils have lower maximum lift coefficients ($C_{L_{\max}}$); therefore, to produce the required thrust in hover, the rotor solidity must increase. A second approach is to add blade sweep which reduces the effective chordwise Mach numbers. However, swept blades at high speeds demonstrate significant aeroelastic instabilities [5]. Therefore, an ideal combination of planform, twist, airfoils and sweep is necessary to achieve improved aerodynamic performance without introducing substantial weight penalties and aeroelastic instabilities. The use of formal optimization procedures, therefore, seems appropriate in such designs. Although a significant amount of research has been performed in applying these techniques for the design of helicopter rotors [6–8], their application in tilt rotor designs is relatively new.

Johnson *et al.* [9] performed a detailed study on the performance, maneuverability and stability of high-speed tilting proprotor aircraft, including the XV-15 and the V-22. Liu and McVeigh [10] recently studied the use of highly swept rotor blades for high-speed tilt rotor use. Benoit and Bousquet [11] performed a parametric study to investigate the proper choice of airfoil selection for improved aerodynamic performance. However, formal optimization techniques were not applied.

The work was supported by NASA Ames Research Center, under Grant NAG2-771, Technical Monitor, J. F. Madden, III.

Recently, Chattopadhyay *et al.* [12–15] have initiated the development of strategies for addressing this complex aircraft design. The high speed propulsive efficiency was maximized with constraints on dynamic, aerodynamic, aeroelastic and structural requirements by Chattopadhyay and Narayan [12,13]. The more complex problem of simultaneously maximizing the propulsive efficiency in high speed cruise and the rotor figure of merit in hover with multidisciplinary constraints have been addressed by [14,16]. The problems were formulated using multiple objective function formulation techniques. The drive system weight is also a critical design issue in the design of the tiltrotor aircraft. Therefore, in [15], Chattopadhyay *et al.* addressed the problem of minimizing the drive system weight using aerodynamic design variables such as twist and RPM.

In this paper, an optimization procedure is developed with the coupling of structures and aeroelastic design criteria. Composite structures, which combine stiffness flexibility and bending-torsion coupling, are ideal for providing superior light-weight structure and composite Advanced Technology Blades (ATB) are currently being used in the XV-15 tiltrotor aircraft [17]. The benefits of composite structures for aeroelastic tailoring of helicopter rotor blades, using formal optimization techniques, has been recognized. Reviews of the use of composite structural models, for rotary wing applications are presented by [18,19]. Friedmann *et al.* [20] developed a completely anisotropic composite model to investigate the aeroelastic stability of rotor blades with both straight and swept tips. A finite element algorithm was used to model the composite beam and both cubic and quadratic interpolation polynomials were used. Ganguli and Chopra [21] also performed an aeroelastic optimization of helicopter rotor blades using an analytical composite box beam model [22]. McCarthy and Chattopadhyay [8] recently used the composite box beam model of [22] within a multidisciplinary optimum design problem of helicopter rotor blades. A similar model is used in this paper to model the load carrying spar inside the airfoil.

2. PROBLEM STATEMENT

An optimization procedure is developed for the design of high speed prop-rotors to be used in civil tiltrotor applications. The goal is to couple structural and aeroelastic stability design requirements inside a closed-loop optimization procedure. The objective is to minimize the total system weight, which includes contributions from the engine, the transmission, the fuel and the rotor blades. Constraints are imposed on rotor blade aeroelastic stability in both hover and high-speed (400 knots) cruise. Both structural and aerodynamic design variables are used.

3. OPTIMIZATION FORMULATION

The optimization problem can be mathematically posed as follows.

$$
\begin{array}{lllll}
\text{Minimize} & F_k(\varphi_n) & k = 1, 2, \ldots, NOBJ & \text{(objective functions)} \\
 & & n = 1, 2, \ldots, NDV & \\
\text{subject to} & g_j(\varphi_n) \leq 0 & j = 1, 2, \ldots, NCON & \text{(inequality constraints)} \\
 & \varphi_{n_L} \leq \varphi_n \leq \varphi_{n_U} & & \text{(side constraints)}
\end{array}
$$

where $NOBJ$ denotes the number of objective functions, NDV is the number of design variables and $NCON$ is the total number of constraints. The subscripts L and U represent lower and upper bounds, respectively, on the design variable φ.

4. ANALYSIS AND OPTIMIZATION

In this section, a description of the analysis procedures, coupled within the optimization process is provided. This is followed by a description of the optimization procedure.

Structural Analysis

The structural analysis of the rotor blade is performed using a recently developed inhouse code. The code models a symmetric single cell composite box beam, which is assumed to carry all loads within the rotor. It is assumed that the flatwise, chordwise and torsional stiffnesses of the blade are provided solely by the box beam.

Dynamic, Aerodynamic and Aeroelastic Analyses

The program CAMRAD/JA [23] is used for blade dynamic, aerodynamic and aeroelastic stability analyses. The blade is trimmed within CAMRAD/JA at each cycle so that the intermediate designs, which are feasible designs, represent trimmed configurations. A wind tunnel trim option is used and the rotor is trimmed to a specific C_T/σ values (C_T is the coefficient of thrust and σ is the area-weighted solidity of the rotor) using the collective blade pitch. The aeroelastic stability analysis is performed using the constant coefficient technique as implemented in CAMRAD/JA. Fifteen bending degrees of freedom, nine torsional degrees of freedom and two gimbal degrees of freedom are used.

Optimization Implementation

The basic algorithm used is the method of feasible directions as implemented in the optimization program CONMIN [24]. The optimization is to be coupled with a comprehensive analysis code. The blade is to be trimmed at each step of design optimization such that each feasible design (i.e., a design that satisfies all constraints) produced by the optimizer represents a trimmed configuration. Since the optimization process requires many evaluations of the objective function and constraints before an optimum design is obtained, the process can be very expensive if full analyses are made for each function evaluation. The objective function and constraints are therefore approximated by an approximation technique which is described below.

Approximation Technique

A two-point exponential approximation [25] is used for approximation of the objective functions and the constraints. This technique takes its name from the fact that the exponent used in the expansion is based upon gradient information from the previous design point. This technique is formulated as follows.

$$\hat{F}(\Phi) = F(\Phi_0) + \sum_{n=1}^{NDV} \left[\left(\frac{\Phi_n}{\Phi_{0_n}} \right)^{p_n} - 1.0 \right] \frac{\Phi_{0_n}}{p_n} \frac{\partial F(\Phi_0)}{\partial \Phi_n}, \tag{1}$$

where

$$p_n = \frac{\ln \left\{ \dfrac{\dfrac{\partial F(\Phi_1)}{\partial \Phi_n}}{\dfrac{\partial F(\Phi_0)}{\partial \Phi_n}} \right\}}{\ln \left(\dfrac{\partial F(\Phi_1)}{\partial \Phi_n} \right)} + 1.0. \tag{2}$$

The quantity Φ_1 refers to the design variable vector from the previous iteration and the quantity Φ_0 denotes the current design vector. A similar expression is obtained for the constraint vector. The exponent p_n can be considered as a "goodness of fit" parameter, which explicitly determines the trade-offs between traditional and reciprocal Taylor series based expansions (also known as a hybrid approximation technique). It can be seen from (2) that in the limiting case of $p_n = 1$, the expansion is identical to the traditional first order Taylor series, and when $p_n = -1$, the two-point exponential approximation equates to the reciprocal expansion form. The exponent is then defined to lie within this interval, such that if $p_n > 1$, it is set identically equal to one, and if $p_n < -1$, it is set equal to -1.

5. BLADE MODELING

The formulation and modeling assumptions used in the integrated optimization problem are described in this section.

Aerodynamic Model

The aerodynamic lifting line offset, from reference axis, is based on a cubic model (Figure 1) with in-plane curvature as follows.

$$x_{ac}(\bar{y}) = \varepsilon_1(\bar{y} - y_{\text{hinge}}) + \varepsilon_2(\bar{y} - y_{\text{hinge}})^2 + \varepsilon_3(\bar{y} - y_{\text{hinge}})^3, \tag{3}$$

where ε_1, ε_2 and ε_3 are constants that determine the curvature, $\bar{y}$ is the nondimensional radial location and y_{hinge} is the hinge offset. The curvature parameters, $\varepsilon_i (i = 1 - 3)$, are defined such that

$$|\varepsilon_i| < \zeta_i, \tag{4}$$

where ζ_i are prescribed bounds for the curvature parameters. These bounds allow for either forward or backward in-plane curvature. When these parameters are equal to zero, the lifting line will be a straight line. Based upon this quadratic lifting line, the sweep variation, in degrees, is calculated as follows.

$$\begin{aligned} \Lambda(\bar{y}) &= \frac{d}{d\bar{y}}\left(x_{ac}(\bar{y})\right) \\ &= \frac{180}{\pi}\left(\varepsilon_1 + 2\varepsilon_2\bar{y} + 3\varepsilon_3\bar{y}^2\right). \end{aligned} \tag{5}$$

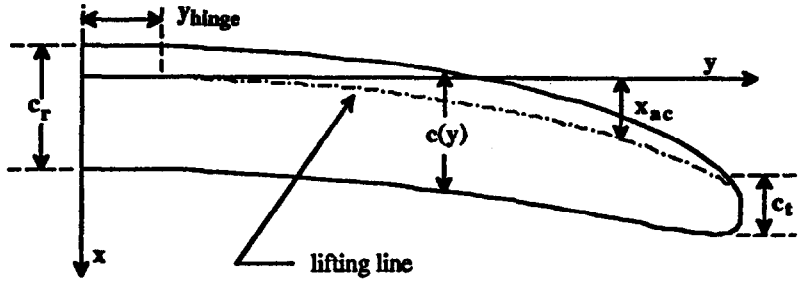

Figure 1. Blade model.

The twist angle of attack, $\theta(\bar{y})$, is defined to have the following spanwise variation.

$$\theta(\bar{y}) = \theta_{\text{ideal}} + \theta_{\text{perturbation}}, \tag{6}$$

where θ_{ideal} is the ideal twist in hover, given by

$$\theta_{\text{ideal}} = \tan^{-1}\left(\frac{V_\infty}{\Omega y}\right), \tag{7}$$

where V_∞ represent the free stream velocity and Ω is the rotor RPM. The quantity $\theta_{\text{perturbation}}$ is defined to have the following spanwise variation

$$\theta(\bar{y}) = \theta_1(\bar{y} - 0.75) + \theta_2(\bar{y} - 0.75)^2 + \theta_3(\bar{y} - 0.75)^3. \tag{8}$$

It is important to note that (8) represents a perturbation from the ideal twist and the values for these coefficients are based upon a previously formulated optimization problem in which the twist was used as a design variable [14].

Structural Model

The load carrying structural member is a single cell composite box beam (Figure 2) symmetric about the x and z axes. The beam is modeled with unequal vertical and horizontal wall thicknesses, and the beam cross section is described by stretching, bending, twisting, shearing and torsion related warping. The box beam walls are made of layers of laminated orthotropic composite plies. A symmetric ply arrangement of $(90°/45°/0°/-45°)_s$ is used for the horizontal walls and a symmetric arrangement of $(0°/\pm 45°/0°)_s$ is used for the vertical walls. The spanwise thickness distribution, $t(y)$, for each ply is based on the following spanwise distribution.

$$t(\bar{y}) = t_0 + t_1\bar{y} + t_2\frac{1}{\bar{y}} + t_3\frac{1}{\bar{y}^2}, \tag{9}$$

where $t_0 - t_3$ are coefficients that determine the thickness distribution. The total thickness of an individual ply with orientation $\Psi(t_\Psi)$ is calculated as follows:

$$t_\Psi(\bar{y}) = n_\Psi t(\bar{y}), \tag{10}$$

where n_Ψ denotes the total number of plies with orientation Ψ. The stiffnesses are calculated based on the formulations presented in [22].

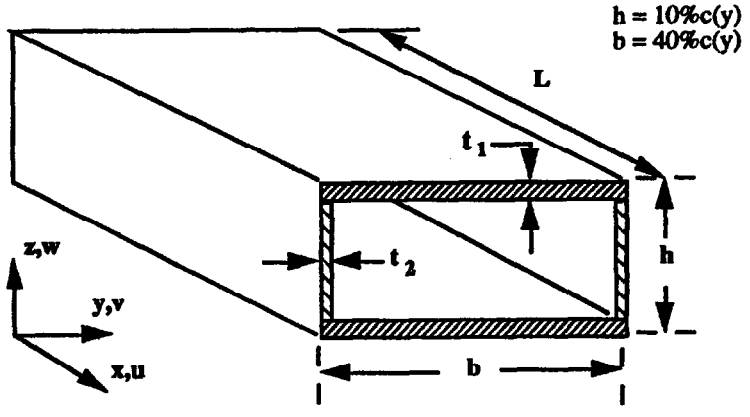

Figure 2. Single cell composite box beam.

Nonstructural tuning weights, $w(\bar{y})$, are placed at the leading edge and the following cubic spanwise distribution is assumed:

$$w(\bar{y}) = w_0 + w_1\bar{y} + w_2\bar{y}^2 + w_3\bar{y}^3, \tag{11}$$

where $w_0 - w_3$ are the coefficients describing the weight distribution. The total blade weight comprises the weight of the box beam, the tuning weights, the skin and the honeycomb weight (used in the trailing edge section).

Objective function

The objective function to be minimized is the perturbation weight difference between the blade weight with composite box beam added and the baseline blade weight. This objective function takes the following form.

$$\text{Min } \triangle W_{\text{blade}} = W_{\text{composite}} - W_{\text{reference}}, \tag{12}$$

where $W_{\text{composite}}$ is the weight of the blade with the composite box beam and $W_{\text{reference}}$ is the weight of the baseline blade.

Design variables

Both structural and aerodynamic design variables are used during the optimization to provide the optimizer with greater flexibility. The structural design variables consist of the composite ply thicknesses and the nonstructural tip weights. The aerodynamic variables used are the blade sweep and the rotational velocity of the rotor in forward flight. A summary of these design variables follows.

(i) Thickness distribution parameters, $t_0 - t_3$.
(ii) Individual ply thicknesses, n_Ψ.
(iii) Nonstructural mass distribution parameters, $w_0 - w_3$.
(iv) Sweep parameters, $\varepsilon_1 - \varepsilon_3$.

Constraints

In order to ensure that the blade is aeroelastically stable in both hover and high speed forward flight, the stability roots for both flight conditions are constrained to be negative. These constraints take the following form.

$$\text{(i)} \quad \alpha_{k_i} \leq 0, \quad k = 1, 2, \ldots, \text{NMODE}, \quad i = 1, 2 \quad (1 - \text{hover}, 2 - \text{axial}),$$

where NMODE is the total number of stability considered in each flight condition.

6. RESULTS

The rotor used, as a reference, is an advanced three bladed prop-rotor with a gimbaled hub. The blade radius is 12.5 feet. The rotor was designed for a cruise speed of 300 knots. The blade is discretized into 51 structural stations and 21 aerodynamic stations. A total of 52 stability modes (NMODE) are considered in both hover and cruise, so that there are 104 constraints. Using a wind tunnel trim option, the optimum rotor is trimmed to C_T/σ value that corresponds to an aircraft lift-to-drag ratio (L/D) of 5.3. This along with the fact that the solidity (σ) of the rotor is held fixed during optimization ensures that the optimized rotor retains the same thrusts as the reference configuration. The optimization is performed at a cruise velocity of 400 knots at an altitude of 25,000 feet above sea level and a rotational velocity of the rotor is $\Omega = 564$ RPM (tip speed of 738 ft/s). The hover analysis is performed at sea level with a rotational velocity of $\Omega = 570$ RPM (tip speed of 746 ft/s). A uniform inflow model is used in both the hover and axial analyses. The material used for the composite box beam is T300/5208 Graphite Epoxy with a volume fraction of 70 percent.

A summary of the optimum results is presented in Tables 1 and 2 and Figures 3–11. From Table 1, it can be seen that there are drastic changes in the design variables from reference to optimum blade. The optimum blade is 21 lbs heavier than the reference rotor, which is an unstable blade in both hover and axial flight. It should be noted, however, that although the weight of each blade of the three-bladed rotor is increased by 21 lbs, a calculation of the drive system weight shows a reduction of 127 lbs from reference to optimum [14]. Therefore, the actual rotor weight is reduced by 67 lbs during optimization although the drive system weight is not included in the form of objective functions or constraints in the optimization formulation. The lifting line distributions are presented in Figure 3 where it is seen that the optimum blade is swept back further than the reference blade. The difference in the two sweep distributions is nearly uniform as can be seen from Figure 4. The additional aft sweep of the optimum blade increases the amount of pitch-flap coupling thereby producing the stabilizing effect necessary.

Figure 5 presents the normalized ply thickness distribution. The figure indicates significant reductions in the thickness throughout the blade span. Table 2 presents the individual ply

Table 1. Summary of optimum results.

	Reference	Optimum
Objective function		
Weight, ΔW (lb)	0.0	21.0
Design variables		
Sweep		
ε_1	−0.451	−0.373
ε_2	0.601	0.638
ε_3	0.0	0.00810
Thickness distribution (in)		
t_0	0.800	0.652
t_1	0.00500	0.00335
t_2	0.00500	0.00460
t_3	0.00500	0.00365
Nonstructural weight (lb/ft)		
w_0	0.0	−0.0108
w_1	0.0	0.0000
w_2	0.0	−0.0173
w_3	0.0	0.0108
Drive System Weight (lb)	2404	2277

Table 2. Composite ply root thicknesses.

	Reference	Optimum
	ply thickness (in)	ply thickness (in)
Horizontal wall		
90°	0.0200	0.0212
+45°	0.0200	0.0193
0°	0.0200	0.0200
−45°	0.0200	0.0193
Vertical wall		
0°	0.0200	0.0211
+45°	0.0200	0.0558
−45°	0.0200	0.0558
0°	0.0200	0.0211

thicknesses (at the root) for each ply orientation. It is seen that all of the plies retain very nearly the reference thicknesses (0.02 inches) with the exception of the ±45° ply in the vertical wall. The thickness of this ply is increased by 279 percent. The reason for this large increase is attributed to the large influence of this ply in increasing the torsional rigidity of the blade, which is critical for aeroelastic stability.

The stiffness distributions of the optimum and the reference blades are shown in Figures 6–8. The torsional rigidity (GJ) is presented in Figure 6 where it is seen that there are significant increases throughout the blade span. These increases are most prominent at root to mid-span locations. The flapping stiffness (EI_{zz}) is shown in Figure 7. The optimum blade stiffness is slightly increased from the reference values at the root. These increases are larger at the mid-span, tapering off near the tip. A different trend is observed in the lagging stiffness (EI_{xx}) as is seen if Figure 8. There are slight decreases in the lagging stiffness throughout the blade span, with the reductions being the largest at the mid-span locations. A possible explanation for these trends is as follows. Since the torsional rigidity is critical for aeroelastic stability, it

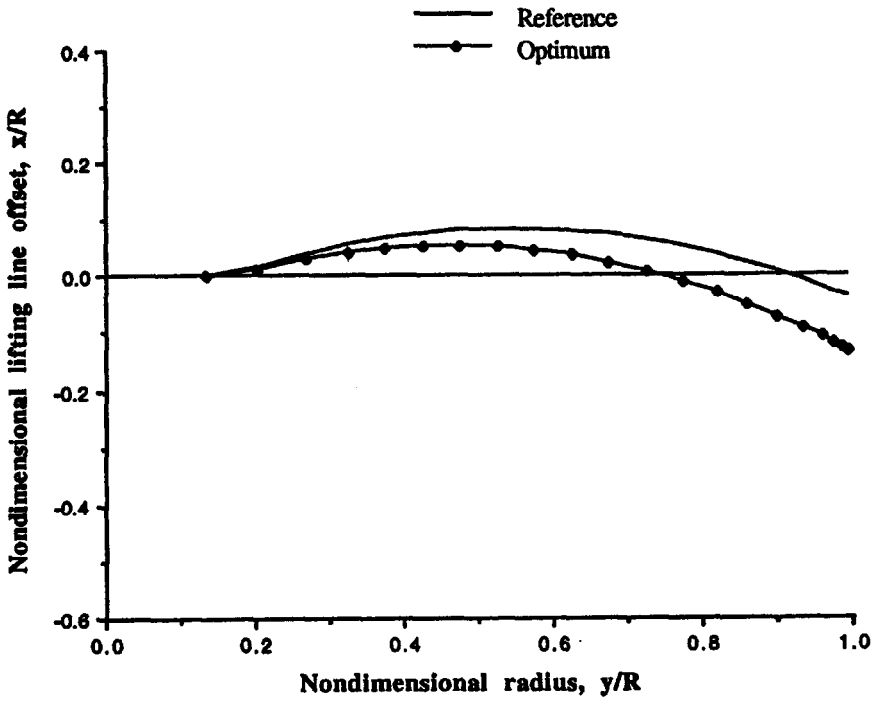

Figure 3. Lifting line distributions.

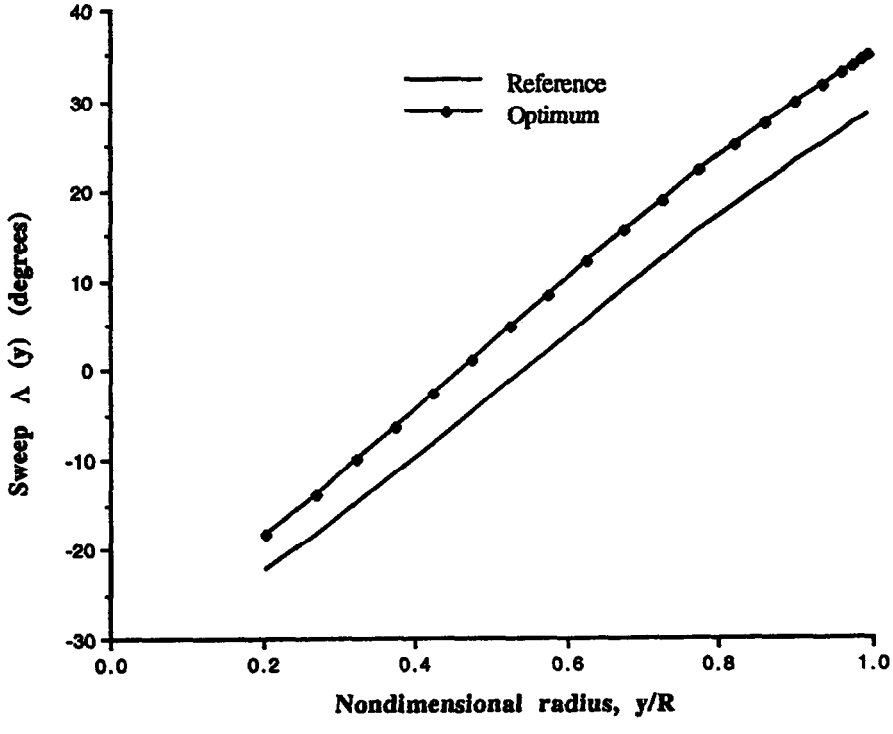

Figure 4. Blade Sweep distributions.

is used as the primary mechanism to ensure that the blades are aeroelastically stable. This is accomplished by dramatically increasing the $\pm 45°$ plies in the vertical wall. This increase then allows the optimizer to decrease the thicknesses of the other plies as a means of weight reduction (the objective function), which in turn reduces the lagging stiffness, but since the lagging stiffness is not as critical as the torsional rigidity, this do not cause aeroelastic stabilities.

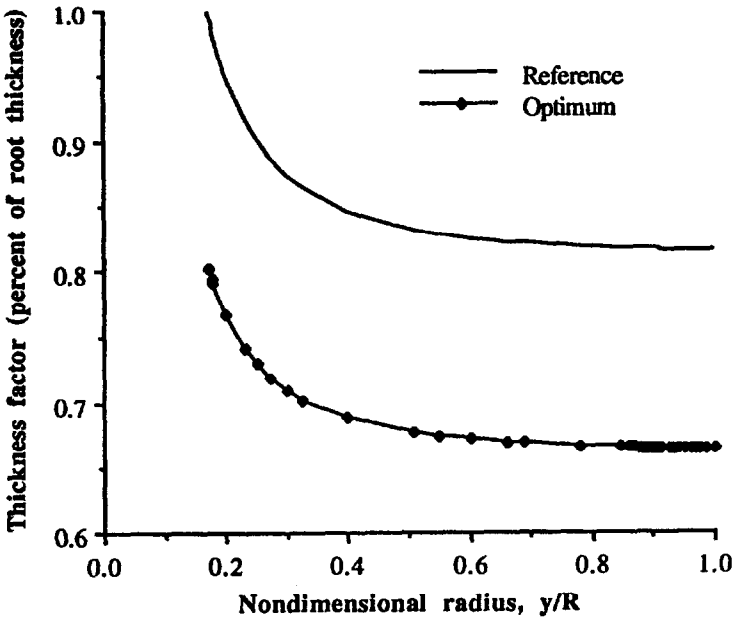

Figure 5. Normalized composite ply thickness distributions.

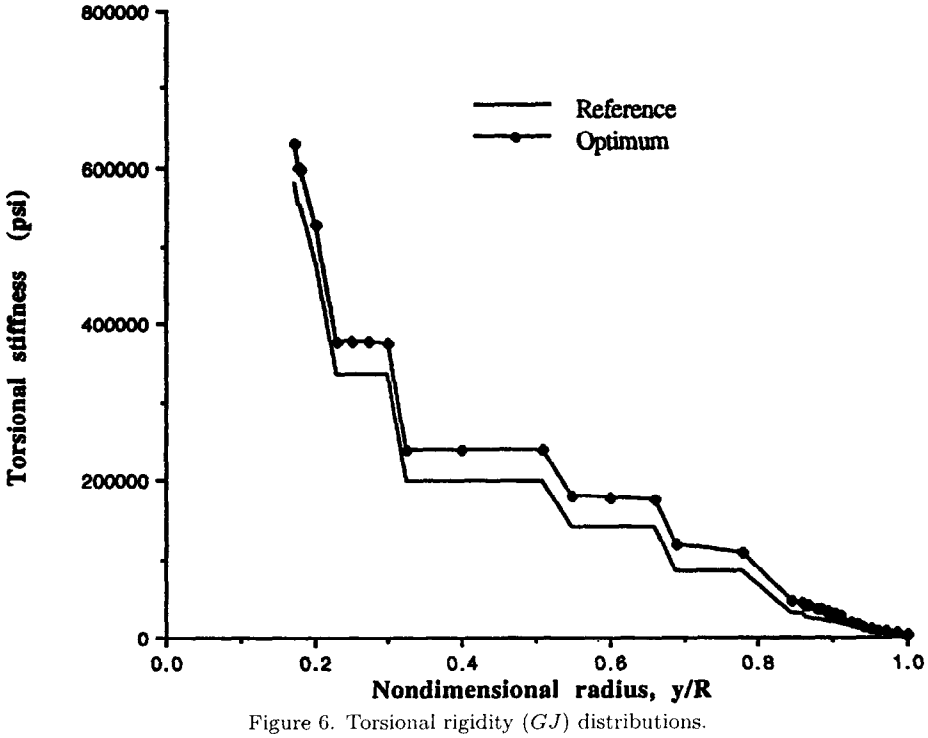

Figure 6. Torsional rigidity (GJ) distributions.

The nonstructural weight per unit length distribution is shown in Figure 9 where it is seen that there is a slight reduction in the nonstructural weights throughout the blade span. These reductions are greatest at the blade tip. These reductions are attributable to the fact that since constraints on the aeroelastic stability are satisfied by increases in the torsional rigidity and the pitch-flap stability of highly swept blade, the optimizer now attempts to reduce the total incremental weight by decreasing the nonstructural weights.

The aeroelastic stability of the reference blade is significantly improved as indicated in Figures 10 and 11 for hover and cruise, respectively. In Figure 10, it is observed that there are six

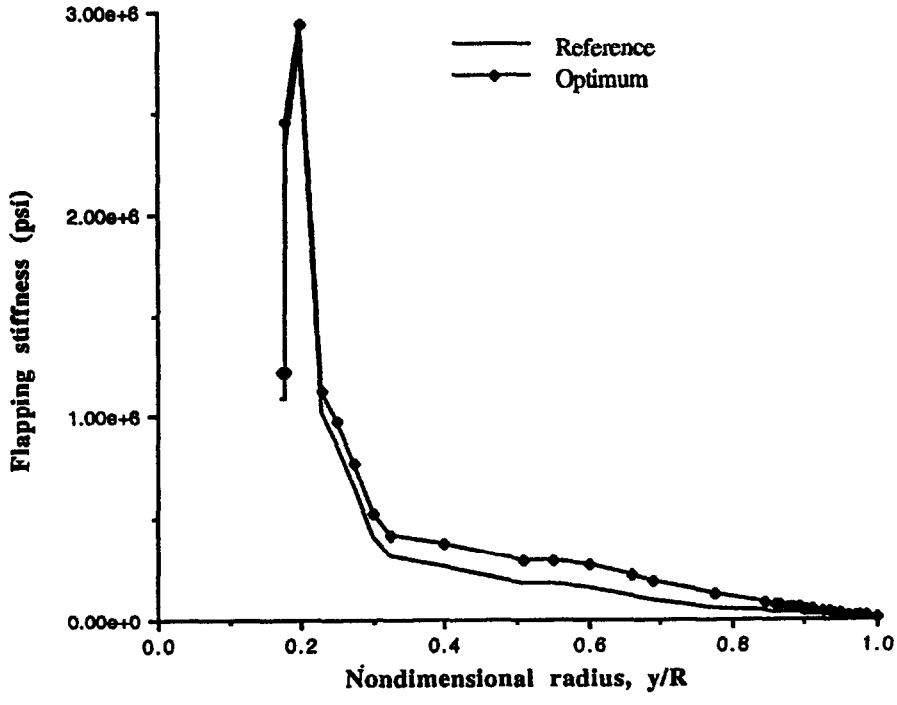

Figure 7. Flapping stiffness (EI_{zz}) distributions.

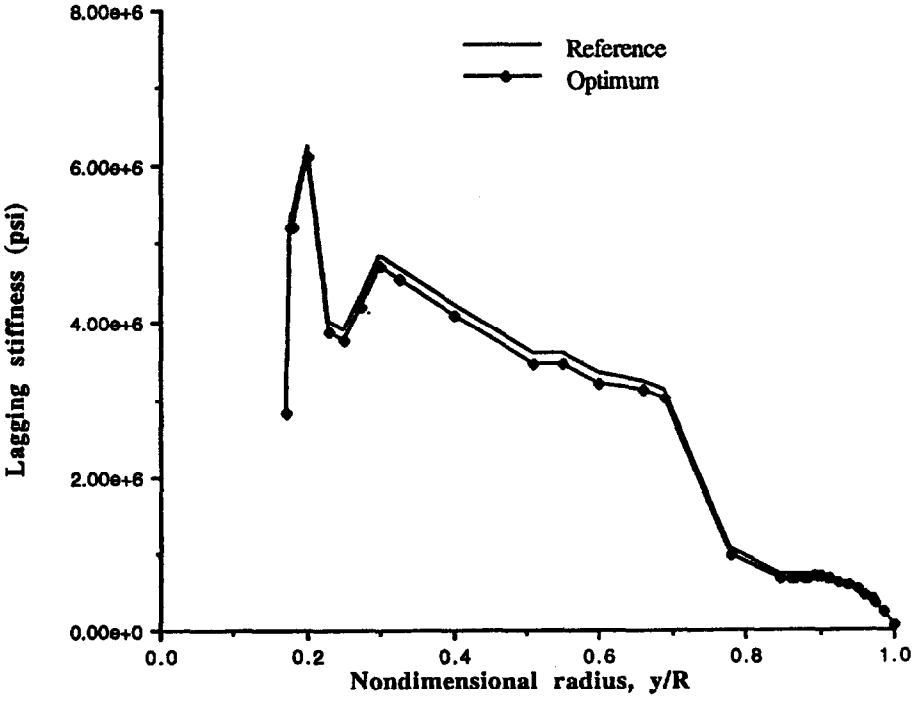

Figure 8. Lagging stiffness (EI_{xx}) distributions.

unstable roots in the reference blade in hover. However, the real part of the stability roots are all positive for the optimum blade indicating a stable system. In cruise (Figure 11), there are eight unstable poles in the reference blade in the axial case, but the optimum rotor is fully stable.

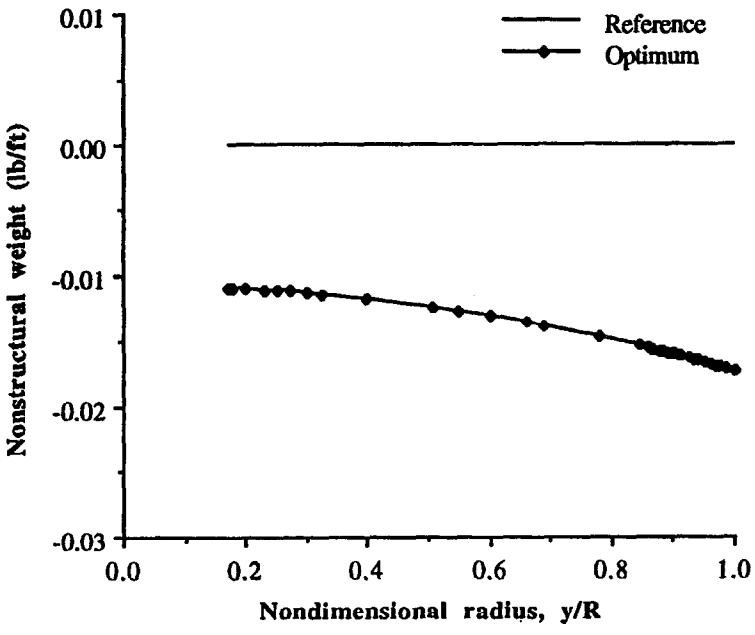

Figure 9. Nonstructural weight distribution.

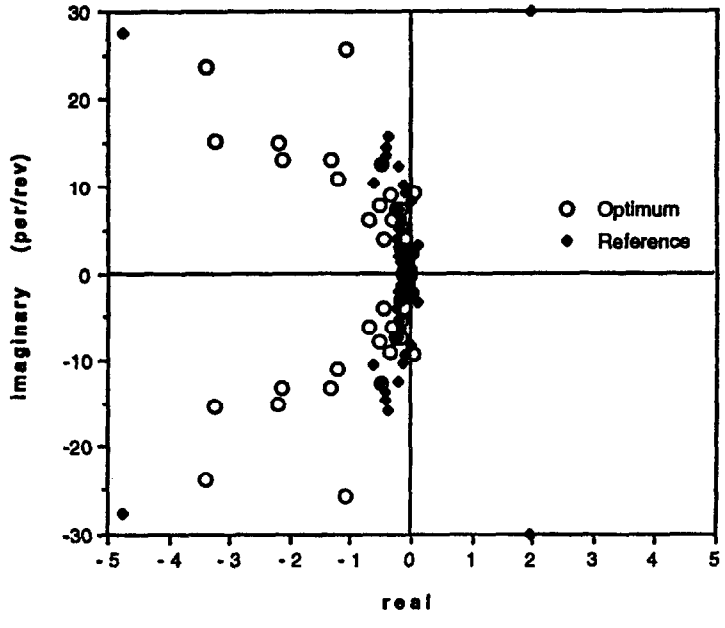

Figure 10. Stability roots in hover.

7. CONCLUSIONS

An optimization procedure is developed with structural and aeroelastic design criteria. The objective function to be minimized is the difference in the blade weight with the pertubational structural model and the reference blade weight. The optimization algorithm used consists of a nonlinear programming technique coupled with an approximate analysis procedure. The results obtained are compared to the reference blade. The following observations are made from this study.

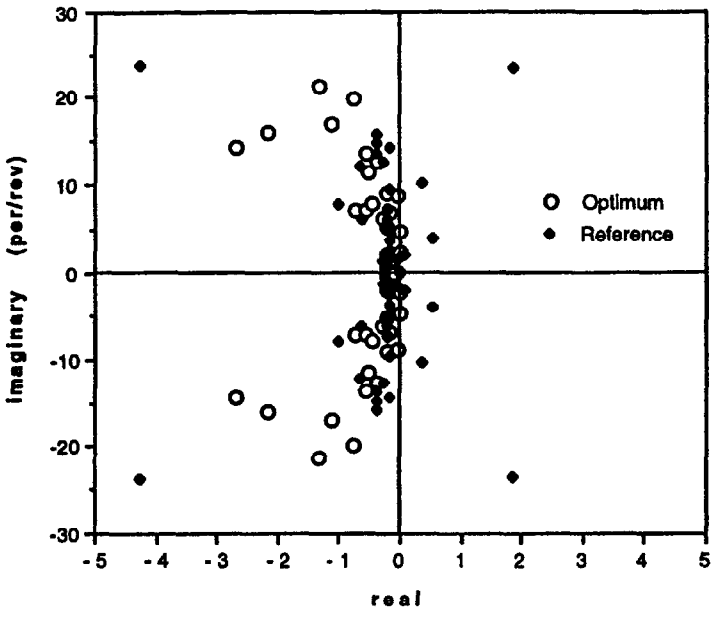

Figure 11. Stability roots in cruise.

(1) Due to the minimum weight objective, the nonstructural weight distribution was used as a primary mechanism for reducing the blade weight, and the torsional rigidity was used as the primary mechanism for improving the aeroelastic stability of the rotor.

(2) The individual optimum blade weight was increased by a small amount from the reference value, as a result of the increased torsional rigidity of the blade which was necessary to make the initially unstable blade aeroelastically stable. However, since the drive system weight was reduced by a large amount during optimization, the total rotor weight reduction was significant.

(3) The optimum blade was more highly aft swept than the reference blade due to the increase in the pitch-flap coupling which has a stabilizing effect on the rotor.

(4) The thickness of the $\pm 45°$ plies in the vertical wall were significantly increased which increased the torsional rigidity of the rotor. The remaining plies remained very nearly equal to the reference thickness.

REFERENCES

1. P. Talbot, J. Phillips and J. Totah, Selected design issues of some high speed rotorcraft concepts, Presented at the *AIAA/AHS/ASEE Aircraft Design, Systems and Operations Conference*, Dayton, Ohio, (Sept. 17–19, 1990).
2. J.B. Wilkerson, J.J. Schneider and K.M. Bartie, Technology needs for high speed rotorcraft (1), *NASA CR 177585* (May 1991).
3. M.W. Scott, Technology needs for high speed rotorcraft (2), *NASA CR 177590* (August 1991).
4. J. Rutherford *et. al.*, Technology needs for high speed rotorcraft, *NASA CR 177578* (April 1991).
5. M.W. Nixon, Parametric studies for tiltrotor aeroelastic stability in high-speed flight, *Proc. 33rd AIAA/ASME/ASCE/AHS Structures, Structural Dynamics, and Materials Conference*, Dallas, Texas, April 13–15, 1992; AIAA paper No. 92-2568.
6. R. Celi and P.P. Friedmann, Structural optimization with aeroelastic constraints of rotor blades with straight and swept tips, *AIAA Journal* **28** (5), 928–936 (May, 1990).
7. J.W. Lim and I. Chopra, Acroelastic optimization of a helicopter rotor, *Proceedings of the 44th Annual Forum of the American Helicopter Society*, Washington, DC, June 1988, pp. 545–558.
8. T.R. McCarthy and A. Chattopadhyay, Multidisciplinary optimization of helicopter rotor blades including design variable sensitivity, Presented at the *Fourth AIAA/USAF/NASA/OAI Symposium on Multidisciplinary Analysis and Optimizations*, Cleveland, Ohio, September, 1992.
9. W. Johnson, B.H. Lau and J.V. Bowles, Calculated performance, stability, and maneuverability of high speed tilting proprotor aircraft, *Vertica* **11** (1987).

10. J. Liu and M.A. McVeigh, Design of swept blade rotors for high-speed tiltrotor application, Presented at the *AIAA Aircraft Design Systems and Operations Meeting*, Paper No. AIAA 91-3147, Baltimore, MD, September 23–25, 1991.
11. B. Benoit and J.M. Bousquet, Aerodynamic design of a tilt-rotor blade, Presented at the *17th ICAS Congress*, September 9–14, 1990, Stockholm, Sweden.
12. A. Chattopadhyay and J. Narayan, Optimum design of high speed prop-rotors using a multidisciplinary approach, Presented at the *48th Annual Forum of the American Helicopter Society*, Washington D.C., (June 3–5, 1992).
13. A. Chattopadhyay and J. Narayan, A design optimization procedure for high speed prop-rotors, *Proc. 33rd AIAA/ASME/ASCE/AHS Structures, Structural Dynamics, and Materials Conference*, Dallas, Texas, April 13–15, 1992; AIAA Paper No. 92-2375.
14. T.R. McCarthy and A. Chattopadhyay, Integrated high speed proprotor optimization, To be presented at the *1993 AIAA/AHS/ASEE Aerospace Design Conference*, Irvine, California, (Feb., 1993).
15. A. Chattopadhyay, T.R. McCarthy and J.F. Madden, A design optimization procedure for minimizing drive system weight of high speed prop-rotors, *Engineering Optimization* (submitted).
16. T.R. McCarthy, An integrated multidisciplinary optimization approach for rotary wing design, Masters Thesis, Arizona State University, (December 1992).
17. S. Lamon, XV-15 advanced technology blade, ultimate stress analysis, *Boeing Report Number D210-12345-1* (1985).
18. P.P. Friedmann, Helicopter rotor dynamics and aeroelasiticity: Some key ideas and insights, *Vertica* **14** (1), 101–121 (1990).
19. D.H. Hodges, Review of composite rotor blade modeling, *AIAA Journal* **28** (3), 561–565 (1990).
20. P.P. Friedmann, C. Venkatesan and K. Yuan, Development of a structural optimization capability for the aeroelastic tailoring of composite rotor blades with straight and swept tips, *Proceedings of the Fourth AIAA/USAF/NASA/OAI Symposium on Multidisciplinary Analysis and Optimizations*, Cleveland, Ohio, September 1992, pp. 722–748.
21. R. Ganguli and I. Chopra, Aeroelastic optimization of a composite helicopter rotor, Presented at the *Fourth AIAA/USAF/NASA/OAI Symposium on Multidisciplinary Analysis and Optimizations*, Cleveland, Ohio, September 1992.
22. E.C. Smith and I. Chopra, Formulation and evaluation of an analytical model for composite box-beams, *Journal of the AHS* **36** (3) (July 1991).
23. W. Johnson, A comprehensive analytical model of rotorcraft aerodynamics and dynamics—Johnson Aeronautics Version, *Vol. II: User's Manual.*
24. G.N. Vanderplaats, CONMIN—A Fortran program for constrained function minimization, *User's Manual, NASA TMX-62282*, (July 1987).
25. G.M. Fadel, M.F. Riley and J.M. Barthelemy, Two point exponential approximation method for structural optimization, *Structural Optimization* **2**, 117–224.